

LATTICE DYNAMICS
AND PHASE TRANSITIONS

Heat Capacity, Structural Disorder, and the Phase Transition in Cryolite $(\text{NH}_4)_3\text{Ti}(\text{O}_2)\text{F}_5$

I. N. Flerov^a, M. V. Gorev^a, V. D. Fokina^a, M. S. Molochev^a, A. D. Vasil'ev^a,
A. F. Bovina^a, and N. M. Laptash^b

^a Kirensky Institute of Physics, Siberian Division, Russian Academy of Sciences,
Akademgorodok, Krasnoyarsk, 660036 Russia
e-mail: flerov@iph.krasn.ru

^b Institute of Chemistry, Far East Division, Russian Academy of Sciences,
pr. Stoletiya Vladivostoka 159, Vladivostok, 690022 Russia

Received November 28, 2005

Abstract—The heat capacity, T - p phase diagrams, and unit cell parameters of cryolite $(\text{NH}_4)_3\text{Ti}(\text{O}_2)\text{F}_5$ were studied over a wide temperature range. A phase transition was found near 226 K, and its thermodynamic characteristics and their dependence on the crystallization conditions were determined. The coordinates and thermal parameters of atoms in the $Fm\bar{3}m$ phase were refined. An analysis of the electron density distribution and the transition entropy showed that the mechanism of the structural transition involves, above all, rotation of the $\text{Ti}(\text{O}_2)\text{F}_5$ octahedra. Possible models of disordering of tetrahedral ammonium groups are considered.

PACS numbers: 77.80.-e; 77.84.Dy; 65.40.Ba

DOI: 10.1134/S1063783406080221

1. INTRODUCTION

Materials belonging to the wide class of oxyfluorides $A_2A'MO_xF_{6-x}$ ($x = 1, 2, 3$) were synthesized and characterized with the x-ray technique at room temperature in [1]. The majority of compounds with atomic cations A and A' ($R_A > R_{A'}$) were found to belong to a cubic elpasolite-like structure with space group $Fm\bar{3}m$ ($Z = 4$), whose frame is formed by fluorine–oxygen octahedra. As regards oxyfluorides with $A = A'$ (cryolites), their structure at room temperature was believed to be distorted and was characterized as pseudotetragonal. Further investigations [2, 3] have shown that both groups of compounds are ferroelectrics at room temperature and, as the temperature increases, they undergo a transition to a paraelectric cubic phase ($Fm\bar{3}m$) as a result of one or two successive structural transitions. In this case, it was suggested that the low-temperature transition is ferroelastic and is caused, at least in cryolites, by ordering processes in the octahedral anion sublattice.

Recent detailed studies of the $(\text{NH}_4)_3\text{MO}_x\text{F}_{6-x}$ compounds ($x = 1.3$, $M = \text{Ti}, \text{W}$) have shown that replacing the spherical cation in the structure of fluorine–oxygen cryolites with a tetrahedral ammonium ion causes the cubic structure to be stable even at room temperature [4, 5].

It is known that the cubic $Fm\bar{3}m$ symmetry can also remain unchanged in related compounds with a seven-coordinated anion. This conclusion has been drawn, in particular, on the basis of numerous room-temperature

studies of the $(\text{NH}_4)_3\text{ZrF}_7$ [6, 7] and $(\text{NH}_4)_3\text{Ti}(\text{O}_2)\text{F}_5$ [8–10] compounds. At the first stage of refining the structure of $(\text{NH}_4)_3\text{Ti}(\text{O}_2)\text{F}_5$ [8], it was supposed that the $3\text{Ti}(\text{O}_2)\text{F}_5^{3-}$ group can be considered a statistically oriented pentagonal bipyramid. Nevertheless, the spatial group $Fm\bar{3}m$ with a disordered distribution of F(O) atoms over four positions (position 96j) was suggested. More detailed studies of this compound [9] revealed that, since the O–O bond is short, the $\text{Ti}(\text{O}_2)\text{F}_5^{3-}$ ionic group is very likely an octahedron. In this case, the O_2^{2-} dumbbell statistically occupies one of the vertices of the octahedron and is oriented in the plane normal to the fourfold axis in two equally probable directions corresponding to the 96j position. According to this model, the fluorine atoms remain ordered and are involved in pronounced anisotropic oscillations around the 24e position.

It was shown in [9, 10] that ammonium cations in interoctahedral voids (position 8c) are ordered, whereas those in the center of the octahedron (position 4b) are disordered. The character of disordering of hydrogen atoms is different in the models proposed in [8] and [9]. In the former model, the H atoms are in position 24e, which corresponds to the ordered state of tetrahedra. In our opinion, this is rather strange, because for cubic symmetry $Fm\bar{3}m$ each tetrahedron in the centers of the octahedra should have at least two equally probable positions, which corresponds to the 32f position for hydrogen atoms. In the model proposed in [9], there are

six equally probable positions of hydrogen atoms (96k). Two of them relate to rotation of the tetrahedra around the twofold axis and three correspond to hydrogen bonds N–H...F(O₂). It should be noted that the authors of [10] have the same point of view regarding the temperature oscillations as the authors of [9].

It would be interesting to estimate the possible entropy changes ΔS in the two different models of the *Fm3m* structure of (NH₄)₃Ti(O₂)F₅ proposed in [8–10] in the case where a phase transition occurs to a completely ordered state. According to [8], the maximum value of ΔS should include the contribution from ordering of the octahedra (each of the five F atoms occupies four equally probable positions, oxygen group O–O occupies two positions), which is equal to $R \ln[(5 \times 4 + 2)/6]$, and the contribution from the ordering of H atoms, which is $R \ln 6/4$. In the model developed in [9, 10], the greatest contribution to the entropy change is due to the ordering of tetrahedra ($R \ln 6$), while the contribution to ΔS made solely by the disordering of the O₂²⁻ group at an octahedron vertex is $\sim(1/6)(R \ln 2)$. However, despite the fact that fluorine atoms are ordered, the contribution to entropy caused by their small displacements in the elpasolite-structure cryolite as a result of the phase transition can be $\sim 0.2R$ according to [11]. For clarity, let us write the values of the phase transition entropy in dimensional units: ~ 14 J/mol K [8] and ~ 17.5 J/mol K [9]. Thus, these significantly different models of the *Fm3m* cubic lattice give relatively close values for the entropy change due to the phase transition to the completely ordered structure. However, this small difference can be reliably detected in heat capacity studies with an adiabatic calorimeter, which makes it possible to determine ΔS of the above-mentioned order of magnitude with an accuracy of 4–6%.

So far, the problem of stability of the cubic phase of the oxyfluoride (NH₄)₃Ti(O₂)F₅ has not been considered, although the fact that this compound has a disordered structure at room temperature suggests that, as the temperature decreases, one or several successive phase transitions can occur with the ordering of building blocks.

In this work, we study the influence of external factors (temperature and pressure) on the behavior of some physical properties of ammonium cryolite (NH₄)₃Ti(O₂)F₅.

2. SYNTHESIS AND CHARACTERIZATION OF SAMPLES

The (NH₄)₃Ti(O₂)F₅ compound was prepared by synthesis from a solution according to the reaction $(\text{NH}_4)_3\text{TiF}_6 + \text{NH}_4\text{F} + \text{H}_2\text{O}_2 = (\text{NH}_4)_3\text{Ti}(\text{O}_2)\text{F}_5 + 2\text{HF}$.

An excess (50 to 100% with respect to the stoichiometric proportion) of NH₄F (40% solution) and then a concentrated (30%) solution of H₂O₂ were added to a

(NH₄)₃TiF₆ solution. As a result, an abundant yellow-lemon deposition of (NH₄)₃Ti(O₂)F₅ formed consisting of fine octahedral single crystals (~ 10 μm in size). After the condensed phase was separated from the solution, bright yellow single crystals with an edge size of 200–1000 μm formed during subsequent slow evaporation in air. In what follows, the crystals obtained at different crystallization stages (slow and fast) will be referred to as *A* (fine) and *B* (coarse) samples.

The compounds thus obtained were certified at room temperature with a DRON-2 x-ray diffractometer. It was found that both types of oxyfluoride (NH₄)₃Ti(O₂)F₅ crystals were cubic (space group *Fm3m*, $Z = 4$) with unit cell parameters that differed insignificantly: $a_0 = 9.2285$ Å (samples *A*) and 9.2367 Å (samples *B*). According to the powder diffraction patterns, no alien phases were found in the samples.

The search for possible phase transitions associated with the disorder of individual atoms in the *Fm3m* structure discussed above was performed at the first stage at low temperatures using a DSM-2M differential scanning microcalorimeter and a powder x-ray diffractometer.

Heat capacity measurements were performed in the temperature range 110–310 K in the heating and cooling modes at a rate of 8 K/min. The sample masses ranged from 0.10 to 0.15 g. The method for determining the heat capacity was the same as that which we used in [12]. The calorimetric studies of both types of samples revealed reproducible heat capacity anomalies, which give evidence of instability of the initial cubic phase. However, it turned out that, although these phase transitions occur at nearly the same temperature, they are characterized by significantly different behaviors of the anomalous heat capacity (Figs. 1a, 1b) and by different values of the thermodynamic parameters. For example, the temperature dependence of the excess heat capacity $\Delta C_p(T)$ that is typical of *A* crystals exhibits an anomaly in the form of a wide “hill” with a sharp peak on the right-hand side. Since the low-temperature part of the heat capacity anomaly does not exhibit the behavior typical of phase transitions, we shall hereafter call the corresponding temperature the temperature of the maximum, $T_m = 203 \pm 4$ K. The anomaly at $T_0 = 225 \pm 2$ K we relate to structural changes caused by a phase transition. This conclusion is also confirmed by the data from polarization-optical studies, according to which the anisotropy and twin structure that were detected at 225 K did not change as the temperature decreased further.

The anomaly in the heat capacity of crystals *B* was observed at a temperature $T_0 = 227 \pm 2$ K and looked like a sharp, almost symmetrical peak. The enthalpies of the respective temperature effects in both crystals were $\sum \Delta H_i = 700$ J/mol (for samples *A*) and $\Delta H_0 = 1800$ J/mol (for samples *B*).

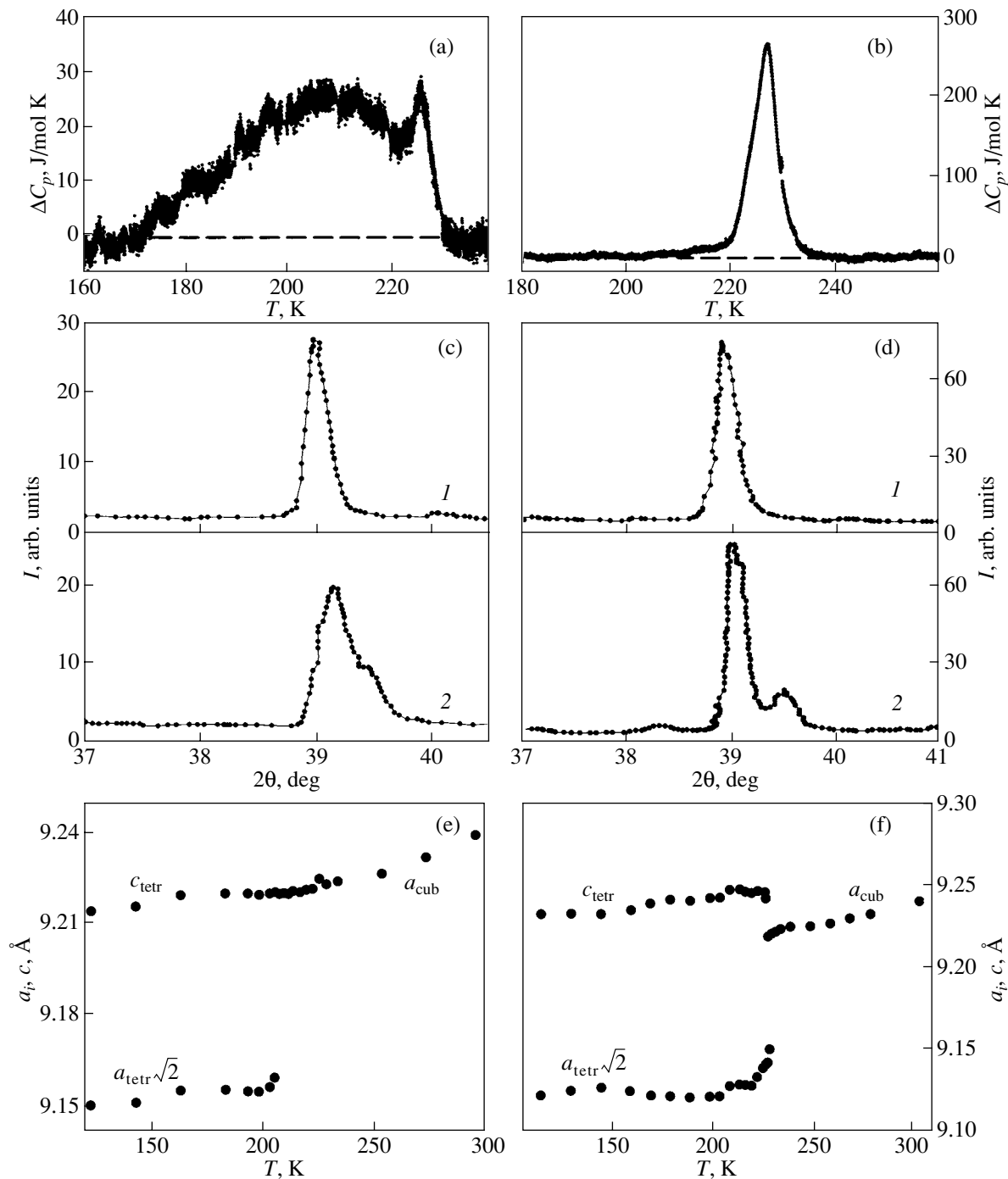


Fig. 1. Results of studying oxyfluoride $(\text{NH}_4)_3\text{Ti}(\text{O}_2)\text{F}_5$: the excess heat capacity of crystals (a) *A* and (b) *B* according to the DSM data; the (400) reflection at (1) 293 K and (2) 123 for crystals (c) *A* and (d) *B*; and the temperature dependence of the unit cell parameters of crystals (e) *A* and (f) *B*.

In the former case, the total enthalpy is given, because we could not split the anomalies at T_0 and T_m .

The occurrence of phase transitions in the $(\text{NH}_4)_3\text{Ti}(\text{O}_2)\text{F}_5$ samples under study was also confirmed by the powder x-ray diffraction patterns obtained in a wide temperature range (120–300 K). In both samples, as the temperature decreases, the low-

symmetry phase manifests itself in broadening and splitting of the $(h00)$ and $(hk0)$ reflections. The typical shape of the (400) reflection for the cubic and distorted phases is shown in Figs. 1c and 1d. It is obvious that a more pronounced splitting of this reflection is typical of crystal *B*. Most lines in the diffraction patterns of the low-temperature phases were identified in terms of the

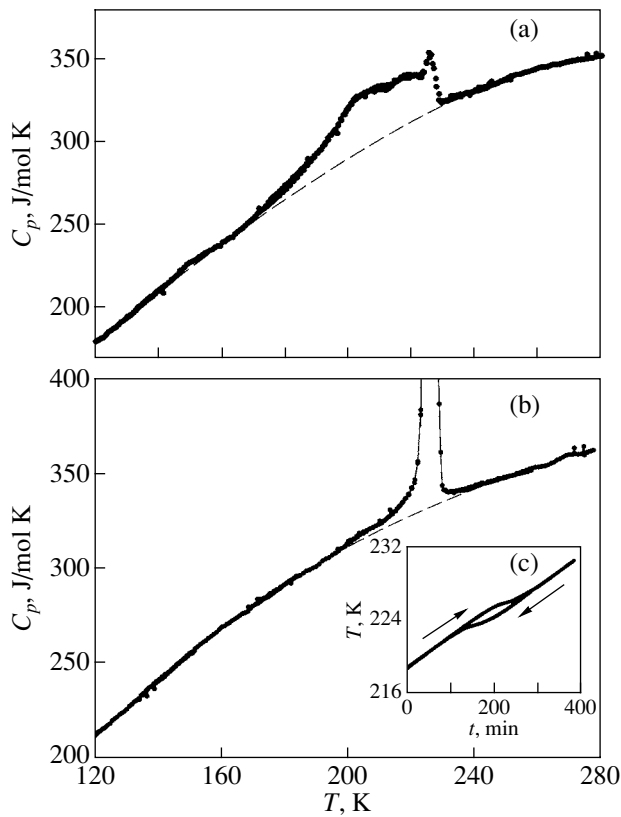


Fig. 2. Temperature dependence of the heat capacity of crystals (a) *A* and (b) *B* of cryolite $(\text{NH}_4)_3\text{Ti}(\text{O}_2)\text{F}_5$ and (c) a thermogram of crystal *B*.

pseudotetragonal unit cell, as was previously done for a $(\text{NH}_4)_3\text{TiOF}_5$ crystal [5]. However, in contrast to the latter crystal, no signs of change in the translation symmetry of the crystal lattice were observed in the x-ray diffraction patterns of $(\text{NH}_4)_3\text{Ti}(\text{O}_2)\text{F}_5$.

The temperature dependencies of the unit cell parameters of $(\text{NH}_4)_3\text{Ti}(\text{O}_2)\text{F}_5$ are shown in Figs. 1e and 1f. An abrupt jump observed in these parameters for both crystals confirms that both samples of this compound undergo a pronounced first-order phase transition. In spite of the fact that two anomalies are observed in the heat capacity of crystals *A*, only one anomaly is observed in the $a_i(T)$ dependence (at T_0). Consequently, crystals *A* undergo one phase transition as do crystals *B*.

However, there is a difference in the behavior of the $a_i(T)$ dependences. In the coarse crystals, the jump is observed for both of these parameters, whereas in the fine crystals the phase transition has almost no effect on the behavior of c .

3. HEAT CAPACITY AND PRESSURE SUSCEPTIBILITY

More detailed heat capacity studies of $(\text{NH}_4)_3\text{Ti}(\text{O}_2)\text{F}_5$ were performed with an adiabatic calo-

rimeter. The samples were tightly pressure-sealed in indium vessels in a helium atmosphere. The sample masses were 0.68 g (samples *A*) and 0.75 g (samples *B*). The measurements were performed over the temperature range 85–280 K in the discrete and continuous heating regimes. The experiment is described in detail in [5].

The results obtained using differential scanning microcalorimetry (DSM) were confirmed in general (Fig. 2). Two anomalies were observed in the heat capacity of crystal *A* at refined temperatures $T_0 = 225.5 \pm 0.5$ K and $T_m = 205 \pm 2$ K, whereas only one anomaly was observed for crystal *B* at $T_0 = 226 \pm 0.05$ K. The heat capacity of the latter crystal was additionally studied near the phase transition temperature using quasi-static thermograms, which were recorded by varying the temperature at a rate $|dT/d\tau| = 4 \times 10^{-2}$ K/min (Fig. 2c). The hysteresis of the phase transition temperature was found to be 1.70 ± 0.05 K.

The regular heat capacity C_L was determined by fitting the experimental data on $C_p(T)$ to polynomials beyond the region of existence of the anomalous contribution to the heat capacity. The excess heat capacity was determined by subtracting the regular contribution from the total heat capacity. The excess enthalpy in $(\text{NH}_4)_3\text{Ti}(\text{O}_2)\text{F}_5$ was calculated by integrating $\Delta C_p(T)$ with respect to temperature over the range 160–240 K (for crystals *A*) or 195–250 K (for crystals *B*) and was found to be $\sum \Delta H_i = 1200 \pm 70$ J/mol and $\Delta H_0 = 2000 \pm 100$ J/mol, respectively. The ratio of the latent heat calculated from the quasi-static thermograms to the total change in enthalpy caused by the phase transition is $\delta H_0/\Delta H_0 = 0.75$ for crystals *B*. This result together with the x-ray data confirms that the phase transition is of the first order and is very far from the tricritical point.

The behavior of the lattice parameters of *A* crystals indicates that the transition from the cubic phase in these crystals is also a well-defined first-order phase transition. From the heat capacity temperature dependence of these crystals (Fig. 2a), it follows that the latent heat, if there is any, can only be related to the anomaly at T_0 . However, this anomaly is small and it is impossible to experimentally prove the presence of δH_0 .

Earlier studies of the T - p diagram of $(\text{NH}_4)_3\text{TiOF}_5$ undergoing one structural transformation at atmospheric pressure [5] revealed that structural distortions in this compound could occur in a stepwise manner. Triple points and pressure-induced phases were observed in the T - p diagram. In order to establish the influence of hydrostatic pressure on the stability of $(\text{NH}_4)_3\text{Ti}(\text{O}_2)\text{F}_5$, both samples of this compound were studied using the DTA method under pressure over the range 0–0.6 GPa. Technical details of these experiments can be found in [5].

It was established that, in the *A* and *B* samples, the temperature at which the loss of stability of the cubic phase occurs increases with pressure at almost the same rate, namely, dT/dp of 40.5 ± 2.0 K/GPa for samples *A* and 44.0 ± 2.0 K/GPa for samples *B* (Fig. 3). The low-temperature anomaly of the *A* sample shifts under pressure very rapidly (at a rate of 212 ± 10 K/GPa), and the two anomalies coalesce near a pressure of 0.15 GPa (Fig. 3a). We do not associate the coalescence of the anomalies with a classical triple point, because in the temperature ranges T_0-T_m and $T < T_m$ the symmetry of the crystal is the same. At higher pressures, the value of dT_0/dp in the *A* sample changes up to 48.7 ± 2.0 K/GPa. No triple points were observed in the T - p phase diagram of *B* the sample (Fig. 3b).

Unfortunately, the structure of the low-temperature phase of $(\text{NH}_4)_3\text{Ti}(\text{O}_2)\text{F}_5$ has not been refined yet, but it is seen from the powder diffraction patterns that this phase is, at least, different from the structure of the distorted phase of $(\text{NH}_4)_3\text{TiOF}_5$ at atmospheric pressure, in which a superstructure was observed [5].

4. X-RAY STUDIES

As mentioned above, the structure of the $(\text{NH}_4)_3\text{Ti}(\text{O}_2)\text{F}_5$ compound was refined several times; however, no consensus on the character of the disordering of fluorine and hydrogen atoms has been reached [8–10]. The significant difference found with calorimetric and x-ray studies between the behaviors of the heat capacity and lattice parameters of *A* and *B* crystals of the same compound obtained by different techniques incited us to reinvestigate, in detail, the structure of the cubic phase in order to refine the coordinates of atoms and the disordering character of, at least, the octahedral groups. Since one of the problems solved in the present work concerns the clarification of the role played by the anion group in the stability of the $Fm\bar{3}m$ structure, x-ray studies were also performed on the $(\text{NH}_4)_3\text{TiOF}_5$ crystal, whose thermodynamic properties we studied previously [5].

The x-ray diffraction patterns of the samples (which were used to refine the crystal structure with the Rietveld technique) were recorded with a D8-ADVANCE diffractometer ($\text{CuK}\alpha$ radiation, θ - 2θ scanning). The scanning step in the 2θ angle is 0.02° , and the exposure at each point is 15 s. In order to decrease the effect of texture on the intensity of reflections, the samples were rotated at a frequency of 0.5 s^{-1} .

The unit cell parameters were determined using the WTREOR software [13] and refined by fitting the profiles using the WINPLOTR software [14]. The main parameters of the data collection and refinement of the structure are listed in Table 1. The space group $Fm\bar{3}m$ is determined by analyzing the extinction of reflections.

The coordinates of the isostructural compound $(\text{NH}_4)_3\text{WO}_3\text{F}_3$ determined in [4] were chosen as the initial parameters for refining the models of all titanates

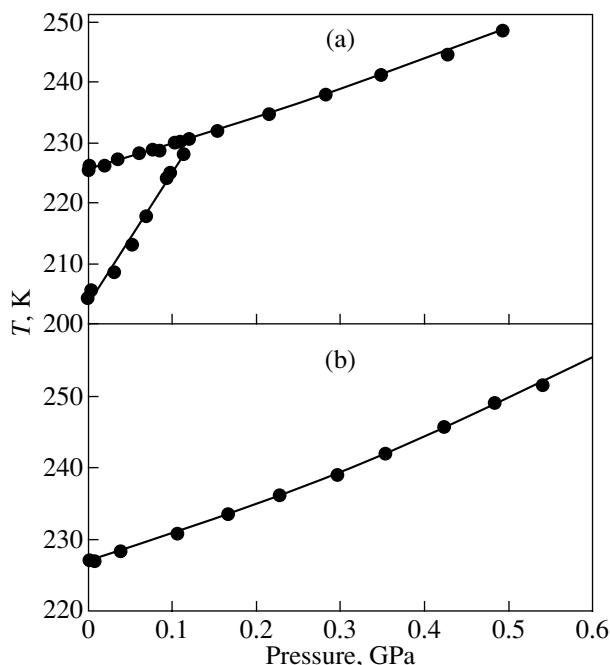


Fig. 3. Phase diagrams of crystals (a) *A* and (b) *B* of cryolite $(\text{NH}_4)_3\text{Ti}(\text{O}_2)\text{F}_5$.

studied in this work. The Ti atom at the center of the octahedron is in the $4a$ position with coordinates (0, 0, 0). The ammonium cations occupy two nonequivalent crystallographic positions: one is in the position $4b$ (0.5, 0, 0) and the two others are in the position $8c$ (0.25, 0.25, 0.25). At the first stage, the F(O) atoms in $(\text{NH}_4)_3\text{TiOF}_5$ were supposed to be located in the position $24e$ with populations of 0.833 (F) and 0.167 (O). The F atom in the $(\text{NH}_4)_3\text{Ti}(\text{O}_2)\text{F}_5$ structure is located on an edge of the unit cell with the same population, 0.833. However, each of the two O atoms, like in [9], was placed in the position $96j$ (0, y , z) under the assumption of forced disordering of the O_2 dumbbell in the cubic unit cell. The latter operation resulted in a significant increase in the reliability factors R . The coordinates of the H atoms and their thermal parameters were fixed. The results of the structural refining of titanium oxyfluorides are summarized in Table 2.

Maps of the electron density distribution over the central cross sections of the TiOF_5 and $\text{Ti}(\text{O}_2)\text{F}_5$ octahedra are shown in Figs. 4a, 4e, and 4i. It is seen that the thermal parameter of the F atoms should be refined following the anisotropic approach. The results of this procedure are shown in Table 3.

5. DISCUSSION OF THE RESULTS

From structural studies of $(\text{NH}_4)_3\text{TiOF}_5$ and $(\text{NH}_4)_3\text{Ti}(\text{O}_2)\text{F}_5$ [4, 8, 9], it follows that the replacement of the TiOF_5 ion group with the more complex $\text{Ti}(\text{O}_2)\text{F}_5$

Table 1. Parameters of data collection and refinement of the structure

Characteristic	(NH ₄) ₃ Ti(O ₂)F ₅ (A)	(NH ₄) ₃ Ti(O ₂)F ₅ (B)	(NH ₄) ₃ TiOF ₅
Space group	<i>Fm3m</i>	<i>Fm3m</i>	<i>Fm3m</i>
a_0 , Å	9.2367(1)	9.22850(6)	9.1090(1)
V , Å ³	788.04(3)	785.947(9)	755.80(2)
Range of angles 2θ, deg	15.00–110.00	15.00–110.00	15.00–110.00
Number of Bragg reflections	46	46	41
Number of refined parameters	9	9	5
R_p	18.6	12.3	15.6
R_{wp}	18.2	14.8	16.5
R_B	5.91	5.71	5.56

Note: a_0 is the unit cell parameter; V is the unit cell volume; and R_p , R_{wp} , and R_B are the profile, weight profile, and Bragg reliability factors, respectively.

Table 2. Coordinates of atoms, isotropic thermal parameters B_{iso} , and position populations p

Atom	p	X	Y	Z	B_{iso} , Å ²
(NH ₄) ₃ TiO ₂ F ₅ (A)					
Ti	1.0	0	0	0	1.50(4)
N(1)	1.0	0.5	0.5	0.5	3.6(2)
H(1)	1.0	0.555	0.555	0.555	1.0
N(2)	1.0	0.25	0.25	0.25	3.1(1)
H(2)	1.0	0.198	0.198	0.198	1.0
F	0.833	0.2057(3)	0	0	5.83*
O	0.0833	0	0.189(1)	0.107(1)	1.2(3)
(NH ₄) ₃ TiO ₂ F ₅ (B)					
Ti	1.0	0	0	0	1.36(4)
N(1)	1.0	0.5	0.5	0.5	3.5(2)
H(1)	1.0	0.56	0.56	0.56	1.0
N(2)	1.0	0.25	0.25	0.25	2.7(1)
H(2)	1.0	0.198	0.198	0.198	1.0
F	0.833	0.2059(3)	0	0	6.9*
O	0.0833	0	0.172(1)	0.102(1)	2.6(4)
(NH ₄) ₃ TiOF ₅					
Ti	1.0	0	0	0	2.34(8)
N(1)	1.0	0.5	0.5	0.5	4.7(4)
H(1)	1.0	0.56	0.56	0.56	1.0
N(2)	1.0	0.25	0.25	0.25	3.4(2)
H(2)	1.0	0.198	0.198	0.198	1.0
F	0.8333	0.2048(4)	0	0	11.1*
O	0.1667	0.2048(4)	0	0	11.1*

* Thermal parameter of the anisotropic model.

group does not change the *Fm3m* cubic symmetry at room temperature.

The calorimetric studies performed in this work on the A and B samples of the (NH₄)₃Ti(O₂)F₅ compound

obtained under different crystallization conditions showed that, in both crystals, the cubic phase becomes unstable and a first-order phase transition occurs as the temperature decreases. The anion substitution

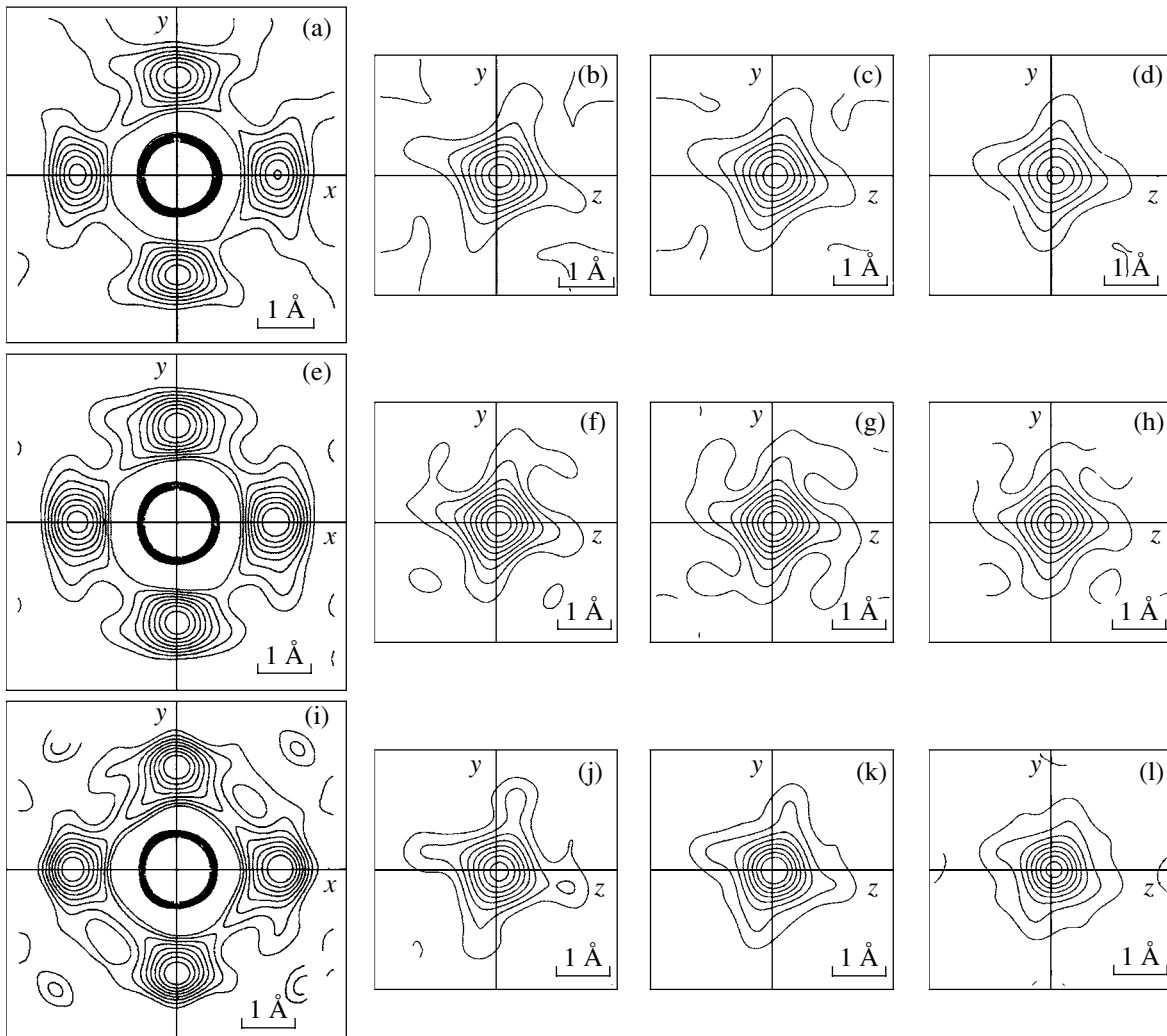


Fig. 4. Electron density cross sections (step $0.4 \text{ electrons}/\text{\AA}^3$) of (a–d) $(\text{NH}_4)_3\text{TiOF}_5$ and (e–l) $(\text{NH}_4)_3\text{Ti}(\text{O}_2)\text{F}_5$ crystals of (e–h) the *A* and (i–l) *B* types. (a, e, i) $z = 0$, and $x =$ (b, f, j) 0.195, (c, g, k) 0.215, and (d, h, l) 0.235.

$\text{TiOF}_5 \rightarrow \text{Ti}(\text{O}_2)\text{F}_5$ results in broadening of the region of existence of the cubic phase (the transition temperature decreases with respect to $T_0 = 264.7 \text{ K}$ in $(\text{NH}_4)_3\text{TiOF}_5$ [5]) and in a change in the symmetry of the low-temperature phase, as follows from the x-ray diffraction and T - p phase diagram studies.

The behavior of the heat capacity and the integrated characteristics of phase transitions in $(\text{NH}_4)_3\text{Ti}(\text{O}_2)\text{F}_5$ samples obtained under different crystallization conditions are very individual. We shall analyze the nature of these distinctions taking into account the fact that the crystallization rate would not be likely to have a significant effect on the firm frame of ion octahedra linked together by shared vertices. This conclusion is favored, for example, by the fact that the temperature T_0 at which the cubic phase becomes unstable and the susceptibility of this temperature to external pressures are virtually the same in the *A* and *B* samples. Therefore, it is expedient to analyze the tetrahedral subsystem.

In the cubic phase of the cryolites studied, the ammonium ions in the $4b$ position should, according to its symmetry, be randomly distributed over two equally probable positions. Thus, the energy potential of oscillations of the tetrahedra has two minima. At high temperatures (about 300 K), the residence time of a tetrahedron in each minimum and the time of its jump between the minima are equal, which corresponds to

Table 3. Anisotropic thermal parameters of F and F(O) atoms

Crystal	$U_{11}, \text{\AA}^2$	$U_{22} = U_{33}, \text{\AA}^2$
$(\text{NH}_4)_3\text{TiO}_2\text{F}_5$ (<i>A</i>)	0.0028(5)	0.0242(5)
$(\text{NH}_4)_3\text{TiO}_2\text{F}_5$ (<i>B</i>)	0.002*	0.0289(6)
$(\text{NH}_4)_3\text{TiOF}_5$	0.0055(6)	0.0476(9)

* Thermal parameter was fixed.

dynamic disorder in the orientations of the ammonium tetrahedron. A decrease in temperature is accompanied by a gradual increase in the population of energy levels, which leads to a Schottky anomaly in the heat capacity curve, i.e., to the appearance of a broad maximum at the temperature T_m [15].

If the structural phase transition takes place at $T_0 > T_m$, both the peak at T_0 and a hill-like anomaly near T_m caused by damping of the rotation of the ammonium groups should appear in the heat capacity curve. If the lattice is distorted (e.g., due to rotation of the octahedra through a small angle), then, according to [11], the corresponding change in entropy will be only $\Delta S_0 \sim 0.2R$. It is this behavior of $C_p(T)$ that we observed in the *A* crystals of the cryolite $(\text{NH}_4)_3\text{Ti}(\text{O}_2)\text{F}_5$. Despite the fact that the temperatures T_m and T_0 are close to each other, we estimated the change in entropy caused by a structural distortion, which appeared to be insignificantly small ($\Delta S_0 \approx 0.7 \text{ J/mol K} \approx 0.1R$), as is typical of phase transitions that involve small rotations of the octahedra.

The coarse crystals of this compound (samples *B*), contrary to the fine crystals (samples *A*), are less stressed, which manifests itself in the different transparencies of the samples found in the optical studies. Stresses, which are most probably nonuniform, can result in significant changes in the character of motion of the tetrahedral groups. It can be suggested that free rotation of the tetrahedra is not probable in the *B* crystals; however, their statistical distribution over two positions in the initial cubic phase is still necessary. Thus, distortion of the structure caused by small rotation of the octahedra and the corresponding reduction of symmetry results in compulsory ordering of the ammonium ions; consequently, a mixed-type phase transition takes place in the $(\text{NH}_4)_3\text{Ti}(\text{O}_2)\text{F}_5$ coarse crystals. The phase transition entropy in this case should be $\Delta S_0 \approx 0.2R + R \ln 2 \approx 7.5 \text{ J/mol K}$, which agrees well enough with the value $\Delta S_0 = 8.92 \pm 0.45 \text{ J/mol K}$ experimentally determined for the phase transition in the *B* samples.

Studies of the T - p phase diagrams show that the temperature T_m increases rapidly in the *A* crystals under pressure and that, above 0.15 GPa, the situation with them becomes similar to that typical of the *B* crystals. Thus, it can be assumed that the difference between some properties of the *A* and *B* crystals is indeed caused by the fact that they are in different nonuniformly stressed states. Attempts to relax stresses by annealing the crystals at 380 K did not change the heat capacity behavior. This might be because the temperature at which the compound decomposes is too low to achieve a relevant change.

The effect we observed is not outstanding. A difference in the behavior of the heat capacity between perovskite-like NH_4MnF_3 and NH_4MnCl_3 crystals containing ammonium was observed in [15, 16]. The change in the unit cell volume due to substitution of halogen

(which can undoubtedly be regarded to be caused by a change in the internal (chemical) pressure) resulted in a change in the ratio of the characteristic temperatures from $T_0 < T_m$ (in NH_4MnF_3) to $T_0 > T_m$ (in NH_4MnCl_3). In the latter case, the $C_p(T)$ dependence is similar to that which we observed in the *A* crystals of $(\text{NH}_4)_3\text{Ti}(\text{O}_2)\text{F}_5$ cryolite. The changes in entropy ΔS_0 also differed significantly depending on the situation: $1.38R$ for NH_4MnF_3) and $0.11R$ for NH_4MnCl_3) [15, 16].

Preliminary results of studying the Raman scattering spectra indicate that the phase transition in the $(\text{NH}_4)_3\text{Ti}(\text{O}_2)\text{F}_5$ samples grown by both crystallization techniques is accompanied by splitting and/or broadening of the lines corresponding to interior oscillations of the octahedra. This result obviously confirms the involvement of the octahedra in the phase transition mechanism. Based on these data, we cannot determine the degree of disordering of the octahedra. However, from the electron density distribution in the octahedra (Fig. 4), it follows that, though oscillations of the F(O) atoms are obviously anisotropic, no atomic disordering is observed. Consequently, the structural distortions can be considered to be actually caused by rotation of the octahedral groups through small angles and correspond to a displacive phase transition.

In view of the above-mentioned structural models and the experimental data on the physical properties, it would be interesting to return to the discussion about the phase transition model in $(\text{NH}_4)_3\text{TiOF}_5$ cryolite, which is characterized by a more considerable change in entropy ($\Delta S_0 = 18.1 \text{ J/mol K} = R \ln 8.8$ [5]) as compared to that in the coarse crystals of $(\text{NH}_4)_3\text{Ti}(\text{O}_2)\text{F}_5$. This fact correlates with the ratio of the root-mean-square displacements of the critical atoms in all the titanates we studied (Table 3) and can, in particular, be related to the experimentally established difference in the symmetries of their low-temperature phases.

In [4], several competing models of the atomic disordering of F(O) atoms in $(\text{NH}_4)_3\text{Ti}(\text{O}_2)\text{F}_5$ were analyzed under the assumption that, in the $Fm\bar{3}m$ phase, the tetrahedra (position $4b$) are disordered in two positions. The preferred variant is $24e + 96j$, for which a complete ordering of the tetrahedra and octahedra results in a change in entropy of $R(\ln 2 + \ln 6) = 20.7 \text{ J/mol K}$. On the other hand, the alternative model that was used to explain the situation in the related cryolites $(\text{NH}_4)_3\text{MF}_6$ ($M = \text{Al, Ga, Fe, Sc}$) [17, 18] and is based on the assumption that the phase transitions (with $\Delta S = R \ln 16 = 23.1 \text{ J/mol K}$) are caused by ordering of the octahedra and tetrahedra disordered in the cubic phase in the eight ($192l$) and two ($32f$) positions, respectively, gives almost the same value of the R factor [4]. Therefore, this model likewise adequately describes the situation in the titanate under study.

Moreover, according to the T - p phase diagram in which high-pressure phases have been found [5], the $Fm\bar{3}m$ phase of the $(\text{NH}_4)_3\text{TiOF}_5$ crystal is character-

ized by a greater degree of disordering than is suggested by the calorimetric data obtained at atmospheric pressure in the temperature range 80–310 K. It cannot be excluded that one more transition exists in this crystal at $T < 80$ K (with ΔS equal to $R \ln 2$ to $R \ln 3$). Consequently, the expected change in entropy caused by complete structural ordering should be in the range $R \ln 16$ to $R \ln 24$. Therefore, the experimental value observed by us, $\Delta S_0 = 18.1$ J/mol K [5], probably corresponds either to the case of complete ordering of the octahedra ($R \ln 8$) or to the case of ordering of the tetrahedra ($R \ln 2$) and partial ordering of the octahedra ($R \ln 4$).

Even though we accepted the models considered for $(\text{NH}_4)_3\text{TiOF}_5$ in [4], the phase transition entropy in this compound can also be found in the model proposed for $(\text{NH}_4)_3\text{Ti}(\text{O}_2)\text{F}_5$, taking into account that the octahedron vertices in $(\text{NH}_4)_3\text{TiOF}_5$ are occupied only by F(O) spherical atoms. One should recall that, in this model, it is suggested that the phase transition is due to small rotations of the octahedra accompanied by ordering of the ammonium groups. So, it could be assumed that the ammonium tetrahedra in the distorted $(\text{NH}_4)_3\text{TiOF}_5$ phase are completely ordered at atmospheric pressure. However, in this case, the phase transition entropy is also small, $\Delta S_0 = 16.6$ J/mol K = $R(\ln 6 + 0.2)$, which is smaller than the experimentally determined value for $(\text{NH}_4)_3\text{TiOF}_5$. One probably cannot exclude that an additional change in entropy (1.5 J/mol K) can be related either to distortions of the octahedra in rotation or to displacements of other atoms (which were observed in oxyfluorides with atomic cations [3]). Thus, this model can be considered only under the assumption of a possible distortion of octahedra. Furthermore, no additional disordering of the cubic phase associated with the possible existence of high-pressure phases in $(\text{NH}_4)_3\text{TiOF}_5$ is envisaged in this model [5].

Thus, it is currently difficult to unambiguously choose a structural model of the cubic phase of $(\text{NH}_4)_3\text{TiOF}_5$ cryolite that can adequately describe the observed thermodynamic properties. Neutron studies of the proton subsystem of the crystal and x-ray studies of the distorted phase structure are required.

ACKNOWLEDGMENTS

The authors are grateful to S.V. Mel'nikova for testing the optical quality of the samples and to A.S. Krylov for supplying information on some details of the Raman scattering studies.

This work was supported by the Krasnoyarsk Regional Science Foundation and the Russian Foundation for Basic Research (project no. 05-02-97707-

r_Yenisei) and by the Siberian Division of the Russian Academy of Sciences (Lavrent'ev Competition of Young Scientists' Projects, project no. 51). V.D.F. is grateful to the National Science Support Foundation for financial support.

REFERENCES

1. G. von Pausewang and W. Rüdorff, *Z. Anorg. Allg. Chem.* **364** (1–2), 69 (1969).
2. G. Peraudeau, J. Ravez, P. Hagenmüller, and H. Arend, *Solid State Commun.* **27**, 591 (1978).
3. J. Ravez, G. Peraudeau, H. Arend, S. C. Abrahams, and P. Hagenmüller, *Ferroelectrics* **28**, 767 (1980).
4. A. A. Udovenko, N. M. Laptash, and I. C. Maslennikova, *J. Fluorine Chem.* **124**, 5 (2003).
5. I. N. Flerov, M. V. Gorev, V. D. Fokina, A. F. Bovina, and N. M. Laptash, *Fiz. Tverd. Tela (St. Petersburg)* **46** (5), 888 (2004) [*Phys. Solid State* **46** (5), 915 (2004)].
6. G. C. Hampson and L. Pauling, *J. Am. Chem. Soc.* **60**, 2702 (1938).
7. H. J. Hurst and J. C. Taylor, *Acta Crystallogr., Sect. B: Struct. Crystallogr. Cryst. Chem.* **26**, 417 (1970).
8. R. Stomberg and I.-B. Svensson, *Acta Chem. Scand., Ser. A* **31**, 635 (1977).
9. W. Massa and G. Pausewang, *Mater. Res. Bull.* **13**, 361 (1978).
10. Ž. Ružić-Toroš and B. Kojić-Prodić, *Inorg. Chim. Acta* **86**, 205 (1984).
11. I. N. Flerov, M. V. Gorev, K. S. Aleksandrov, A. Tressaud, J. Grannec, and M. Couzi, *Mater. Sci. Eng., R* **24** (3), 81 (1998).
12. I. N. Flerov, V. D. Fokina, A. F. Bovina, and N. M. Laptash, *Solid State Sci.* **6**, 367 (2004).
13. P.-E. Werner, L. Eriksson, and M. Westdahl, *J. Appl. Crystallogr.* **18**, 367 (1985).
14. T. Roisnel and A. Rodrigues-Carvajal, in *Proceedings of the Seventh European Powder Diffraction Conference (EPDIC-7), Barcelona, Spain, 2000* (Mater. Sci. Forum, 2000), Vol. 378–381, p. 118.
15. C. Pique, E. Palacios, R. Burriel, J. Rubin, D. Gonzalez, R. Navarro, and J. Bartolome, *Ferroelectrics* **109**, 27 (1990).
16. R. Burriel, J. Bartolome, R. Navarro, and D. Gonzalez, *Ferroelectrics* **54**, 253 (1984).
17. M. V. Gorev, I. N. Flerov, A. Tressaud, D. Denu, A. I. Zaitsev, and V. D. Fokina, *Fiz. Tverd. Tela (St. Petersburg)* **44** (10), 1864 (2002) [*Phys. Solid State* **44** (10), 1954 (2002)].
18. I. N. Flerov, M. V. Gorev, K. S. Aleksandrov, A. Tressaud, and V. D. Fokina, *Kristallografiya* **49** (1), 107 (2004) [*Crystallogr. Rep.* **49** (1), 100 (2004)].

Translated by E. Borisenko